Scripta Materialia 166 (2019) 10–14

Contents lists available at ScienceDirect

Scripta Materialia

journal homepage: www.elsevier.com/locate/scriptamat

Improved cyclic softening behavior of ultrafine-grained Cu with high microstructural stability

P. Xue [a], B.B. Wang [a], X.H. An [b,*], D.R. Ni [a], B.L. Xiao [a], Z.Y. Ma [a,*]

[a] Shenyang National Laboratory for Materials Science, Institute of Metal Research, Chinese Academy of Sciences, 72 Wenhua Road, Shenyang 110016, China
[b] School of Aerospace, Mechanical and Mechatronic Engineering, The University of Sydney, Sydney, NSW 2006, Australia

ARTICLE INFO

Article history:
Received 9 January 2019
Received in revised form 18 February 2019
Accepted 23 February 2019
Available online xxxx

Keywords:
Friction stir processing
Ultrafine-grained Cu
Cyclic softening
Stable microstructures
Low-cycle fatigue life

ABSTRACT

We report that the uniform and stable microstructure essentially ameliorate the cyclic softening of the ultrafine-grained (UFG) Cu prepared by friction stir processing (FSP) and then enhance its low-cycle fatigue properties. In lieu of the fatigue-induced grain coarsening, dislocation and grain boundary (GB) activities play crucial roles in accommodating the cyclic plasticity. In addition, the protrusion and small cracks near the GB regions rather than shear bands are main surface damage morphologies that lead to its final fatigue failure.

Over the last several decades, ultrafine-grained (UFG) and nanostructured (NS) materials processed by severe plastic deformation (SPD) have been extensively investigated owing to their unique microstructures and excellent mechanical properties [1,2]. It is well known that UFG metallic materials possess ultrahigh strength and hardness, while the saturated crystal defect induced by SPD and very fine grains limit their strain hardening capability, leading to a disappointingly low ductility [1,2]. Many efforts have been made to improve the strength-ductility combination of UFG materials through the optimized manipulation of the microstructures [3–7].

In addition to the tensile properties, the cyclic deformation behavior of the UFG material is of crucial significance for the practical engineering applications as well. Generally, compared to their coarse-grained (CG) counterparts, the improved high-cycle fatigue (HCF) strength and the decreased low-cycle fatigue (LCF) lives were obtained in the UFG materials [8]. The deteriorated LCF performance that is one of critical bottleneck restricting the prospective applications of UFG materials can be ascribed to the cyclic softening behavior, which also essentially restricts the further enhancement of their HCF strengths [9].

Previous investigations revealed that the cyclic softening behavior originated from the microstructure instability in terms of grain coarsening and shear banding that are the inherent fatigue damage mechanisms of the UFG and NS materials [8]. The metastable microstructures and non-equilibrium grain boundaries (GBs) produced by SPD enable the easy motion of GBs during long-term to-and-fro deformation, leading to the grain growth, the formation of shear localization and final fatigue failure. Based on the thermal activation nature of the fatigue damage mechanism, low-temperature cyclic deformation and decreasing the stacking fault energy of UFG materials were proposed to stabilize the microstructures and then ameliorate the cyclic softening behavior [10–13], which enhanced the fatigue endurance as well.

Recently, an UFG microstructure prepared by the combination of cold rolling and a proper annealing treatment was developed to surprisingly exhibit higher fatigue limit than conventional UFG materials with higher tensile strengths [14,15]. However, previous investigations generally proposed that mild annealing treatment of the UFG materials which can lead to a "bimodal grain size distribution" also improved the LCF fatigue resistance [5,6,16,17] at the expense of fatigue strength due to the reduction of tensile strengths. In fact, the optimization of the microstructures with recrystallized fine grains and low density of crystal defects, enable the high microstructure stability during fatigue, resulting in the enhancement of fatigue endurance [10–13].

It is well known that friction stir processing (FSP) is an effective method to prepare bulk UFG materials with stable microstructures in terms of equiaxed recrystallized microstructure with low dislocation density and a high ratio of high angle GBs (HAGBs) [18–24]. Our early investigation indicated that the fatigue endurance of the UFG Cu prepared by FSP with relatively low tensile strength is much higher than those obtained by equal channel angular pressing (ECAP) and high-pressure torsion (HPT) [25]. However, it is still uncertain about its cyclic stress response and LCF lives. In this study, strain-controlled LCF tests and various advanced microscopic examinations were performed to

* Corresponding authors.
E-mail addresses: xianghai.an@sydney.edu.au (X.H. An), zyma@imr.ac.cn (Z.Y. Ma).

https://doi.org/10.1016/j.scriptamat.2019.02.040
1359-6462/

primarily explore the cyclic softening behavior, fatigue mechanism, and surface damage.

The commercially pure Cu (99.98 wt%) plates of 3 mm thickness, which was cold rolled (CR) to ~50% thickness reduction, were used in this study. The CR plates were first annealed 2 h at 700 °C, then fixed in water and subjected to FSP at a rotation rate of 600 rpm and a traverse speed of 50 mm/min using a tool with a shoulder 12 mm in diameter. Additional rapid cooling by the flowing water was adopted during FSP [24]. The specimen for tensile and fatigue tests were cut from the processed zone along the FSP direction. The tensile specimens with a gauge section of 5 mm × 1.5 mm × 1.2 mm, were tested at room temperature and a strain rate of 1×10^{-3} s^{-1} on an Instron 5848 tester.

The LCF tests were conducted using specimens with the gauge section of 12 mm × 3 mm × 2.5 mm on an Instron 8871 fatigue testing machine at a strain ratio R of 0.1 (R is defined as $\varepsilon_{max}/\varepsilon_{min}$) and a frequency of 0.5 Hz at room temperature under total strain control. An extensometer with a gauge length of 10 mm was applied to measure and control the strain instantaneously. The microstructure before and after fatigue tests were characterized by scanning electron microscopy (SEM) equipped with electron backscatter diffraction (EBSD), and transmission electron microscopy (TEM). The detailed information about sample preparation and characterization can be found in Ref. 20.

The typical microstructural features of the CR Cu are a high density of low angle GBs (LAGBs) within the coarse grains with an average size of ~20 μm, as shown in the EBSD image of Fig. 1(a), while the kernel average misorientation (KAM) map in Fig. 1(b) reveals the high local misorientation, implying the intergranular rotation introduced by geometrically necessary dislocations. In addition, the TEM image of Fig. 1(c) indicates that many tangled dislocations and ultrafine cells or sub-grains bounded by dislocation walls formed along the rolling direction as marked in Fig. 1(c), which is similar to those after one-pass ECAP processing [26].

In contrast, the microstructural characteristics of the FSP Cu are the uniform equiaxed fine grains with an average size of ~1 μm measured automatically by the EBSD software and there is no preferential texture, as shown in Fig. 1(d). Although dynamic recrystallization dominated the formation of the ultrafine grains, few LAGBs were still detectable in the equiaxed ultrafine grains, which is similar to other FSP materials [18–24,27]. As exhibited in Fig. 1(e), the local misorientation reflected by the KAM map was not homogeneously distributed and is highly related to the dislocation activities or LAGBs, while profuse twin boundaries marked by the red lines formed. TEM image in Fig. 1(f) indicate the formation of ultrafine grains with sharp and clear GBs, and a few wavy and ill-defined LAGBs and dislocations can be observed. Owing to the difference in the resolution capability, the average grain size obtained by TEM that is about 800 nm is generally smaller than that measured by EBSD.

The engineering stress-strain curves of two Cu samples are presented in Fig. S1. For the CR Cu, a high ultimate tensile strength (UTS) of 355 MPa together with a low uniform elongation of only about 2% was obtained, which was similar to those of the UFG Cu prepared by SPD [1]. In contrast, for the FSP UFG Cu, although the UTS was slightly reduced to 320 MPa, the uniform elongation was significantly increased to approximately 12%, implying an enhanced strength-ductility synergy.

Fig. 2(a) shows the dependence of the number of cycles to failure on the cyclic strain range of two Cu samples in a log-log form. Compared to that of the CR Cu, the fatigue life of the FSP UFG Cu is generally enhanced at all cyclic strain ranges, while the improvement is much more prominent at the high cyclic strain ranges. In combination with previous results regarding the fatigue endurance [25], the LCF and HCF properties of the FSP UFG Cu are upgraded simultaneously, which should be highly pertinent to its unique cyclic deformation behavior.

Similar to those obtained by SPD, the decrease in the stress amplitude with cyclic numbers was apparent for the CR Cu at all cyclic strain ranges (Fig. 2(b)), signaling the occurrence of cyclic softening. In contrast, for the FSP UFG Cu, the cyclic softening becomes less significant (Fig. 2(c)), which also can be substantiated by the evolution of cyclic stress-strain hysteresis loops of the two Cu samples at low and high cyclic strain ranges (Fig. S2).

To quantitatively characterize the cyclic softening degree that is an essential indicator of the LCF lives of the UFG materials, the cyclic softening ratios, defined as the ratio of the stress amplitude difference at half fatigue lives and the first cycle to the stress amplitude for the first cycle [10], are calculated and exhibited in Fig. 2(d). Although the cyclic softening ratios of two samples slightly increase with cyclic strain ranges, the cyclic softening ratios for the FSP UFG Cu are much smaller than those for the CR Cu. Such different cyclic softening behavior should be closely related to the microstructural evolution, surface morphology, and fatigue damage mechanisms.

The overall microstructures and surface damage morphology of two Cu samples fatigued at the cyclic strain range of 0.8% are exhibited in Fig. 3. For the CR Cu, the local misorientation became smaller, implying that dynamic recovery happened during the fatigue test. Besides, the distribution of the local misorientation is rather inhomogeneous and it seems that some dislocation configurations formed in several grains (Fig. 3(a)). Very large persistent slip band (PSB) can be clearly observed on the damaged surface of the CR Cu, and the cracks nucleated and propagated along the bands or the GBs (Fig. 3(b)).

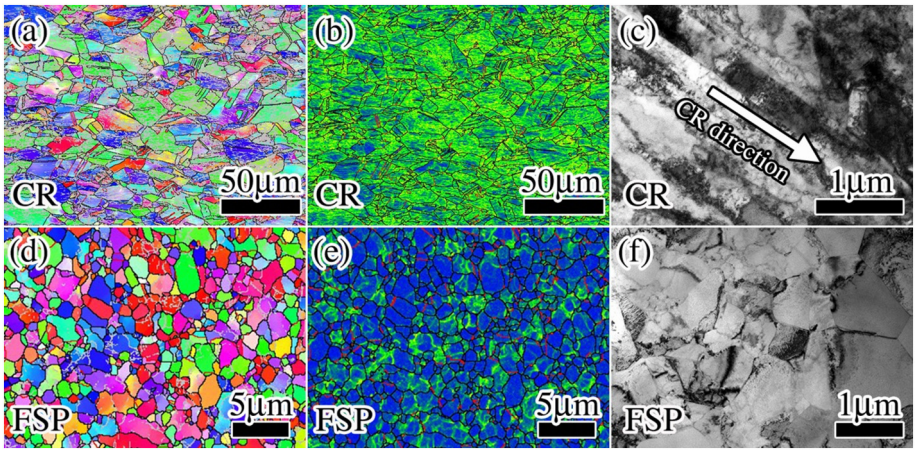

Fig. 1. (a) Inverse pole figure (IPF) map, (b) KAM map and (c) TEM image of CR Cu; (d) IPF map, (e) KAM map and (f) TEM image of the UFG Cu prepared by FSP. In the IPF and KAM map, the black lines, gray lines and red lines represent HAGBs, LAGBs and twin boundaries, respectively. (For interpretation of the references to color in this figure legend, the reader is referred to the web version of this article.)

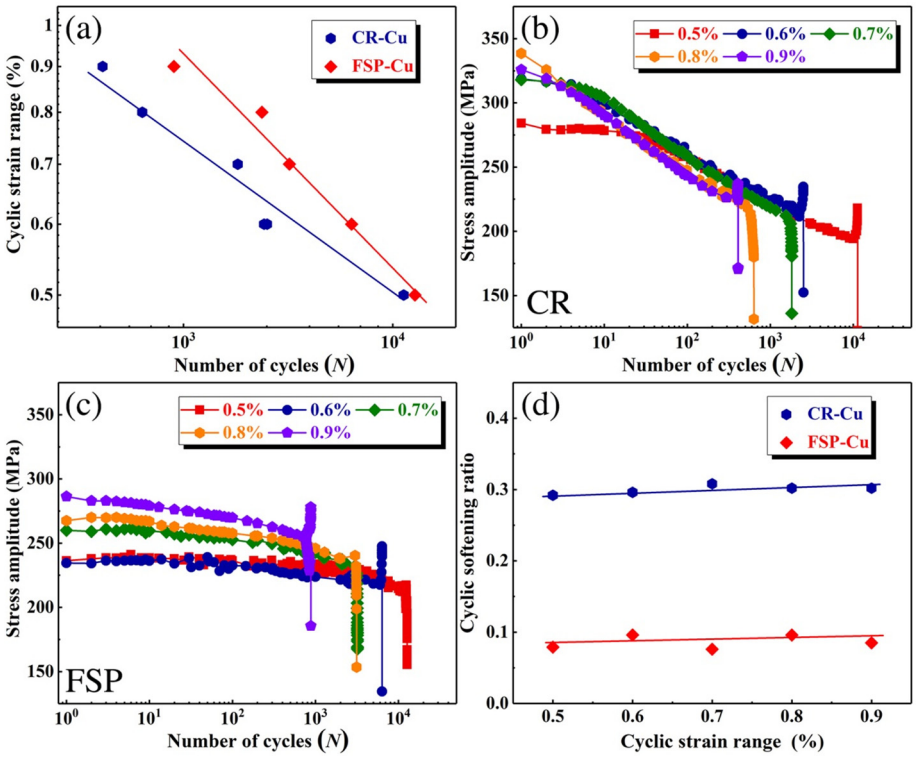

Fig. 2. (a) The relationship between cyclic strain ranges and LCF lives of the CR and FSP Cu samples, (b) and (c) typical stress amplitudes evolution with cyclic numbers of two samples under different cyclic strain ranges, (d) the relationship between cyclic softening ratios and cyclic strain ranges of the CR and FSP Cu samples.

For the FSP Cu, no apparent grain growth was detected, while the change in the local misorientation reflected by KAM map is significant (Fig. 3(c)). Due to the dynamic recovery, local misorientation was generally reduced and exhibited a boundary like distribution in many grains after cyclic deformation. In addition, much smaller SBs rather than large-scale shear bands were observed and confined in some relatively large grains with sizes of about several microns (Fig. 3(d)). Some protrusions and small cracks can be found along the GBs, signaling high pertinence of the fatigue failure to the deformation activities near the GBs even though there is no fatigue-induced grain coarsening.

Fig. 4(a) and (b) displays the representative post-fatigue microstructures of the CR and FSP Cu at the cyclic strain range of 0.8%. For the CR

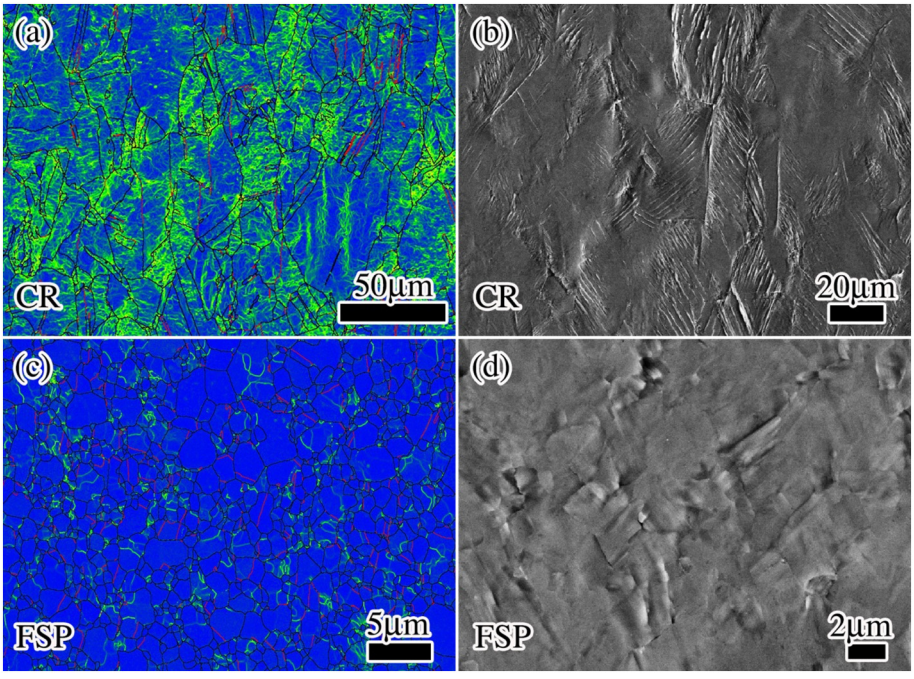

Fig. 3. (a) and (b) KAM map and surface damage morphology of CR Cu, (c) and (d) KAM map and surface damage morphology of FSP Cu, both of which are after fatigue at the cyclic strain range of 0.8%.

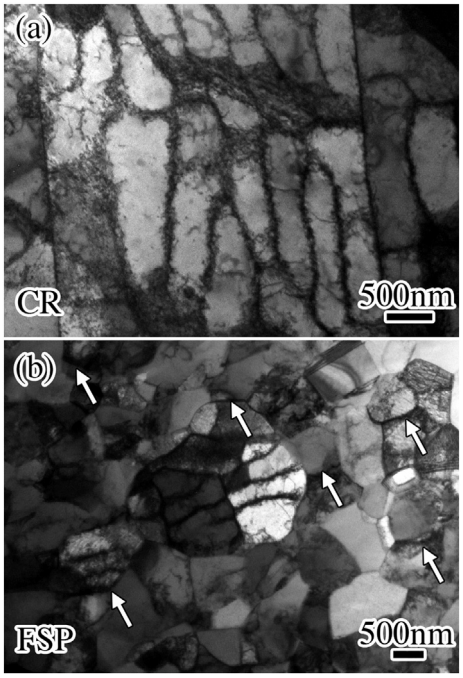

Fig. 4. TEM images showing the post-fatigue microstructure for (a) CR Cu and (b) FSP Cu fatigued at the cyclic strain range of 0.8%.

Cu, fatigue deformation reshaped the microstructures obtained by cold rolling. In lieu of the original elongated dislocation boundaries, various typical dislocation configurations, such as dislocation walls and cells, developed in the various grains (Fig. 4(a)), which is similar to those of fatigued CG Cu [28].

For the FSP Cu, the grain structure almost kept the original morphology without obvious grain growth (Fig. 4(b)). In some large grains, the typical dislocation substructures developed as well, while a high density of dislocations formed in some ultrafine grains since the recrystallized grains can store these crystalline defects. Therefore, dislocation activities played crucial roles in carrying the cyclic plasticity in the UFG Cu. However, the careful TEM inspection revealed dark contrast with a certain width along and near the GB regions as marked by the white arrows, which is distinct from the original sharp GBs before fatigue. This may imply that high cyclic plasticity was accommodated in these regions as well, leading to the formation of protrusions and cracks and final fatigue failure.

As well known, cyclic softening behavior of the UFG materials can be ascribed to the extensive grain coarsening via GB migration, which is highly pertinent to the complicated dislocation activities, like the cross slip, and the strain localization in the shear bands [29–33]. In fact, high density of defects, non-equilibrium GBs, very small grain sizes and large internal stress, all of which are induced by the SPD, are the essential driving forces for the grain growth, leading to the microstructure instability and the cyclic softening [34]. Although the grain growth was not observed in the CR Cu due to its initial large grain size, the cyclic softening should originate from the rearrangement of dislocation substructures through the dynamic recovery, which enables the surface damage to be similar to that of CG Cu.

For the FSP UFG Cu, since the dislocation reorganization through dynamic recovery took place as well, which resulted in the boundary-like distribution of local misorientation (Fig. 3(c)), the stress amplitudes still decreased slightly with the number of cycles during fatigue. However, UFG microstructures prepared by FSP developed through the dynamic recrystallization [18], which enables the UFG materials to possess a low density of defects, relatively stable GBs, moderate grain sizes and small internal stress. All of these benign microstructural features significantly suppress the grain coarsening and then intrinsically render the high microstructure cyclic stability of the UFG materials. Besides, the formation of plenty twin boundaries with low energy during FSP is extremely beneficial to stabilize the microstructures during fatigue [35,36]. Therefore, the cyclic softening behavior is remarkably improved in the FSP UFG Cu with high microstructure stability, which enables the enhancement of its LCF lives.

Recent investigations revealed that the local grain growth in the UFG materials during fatigue led to the high stress/strain incompatibility and thus significantly promoted the strain localization [34,37]. Herein, the relatively uniform microstructures and high structural stability in the FSP UFG Cu essentially suppressed the formation of the shear band, which is also the typical characteristic of the cyclic softening. Instead, slip bands formed in some relatively large grains and the fatigue failure seems to stem from the GB regions as shown in Figs. 3(d) and 4(b). Apart from the extensive interaction between dislocations and GBs, the areas with a certain width and dark contrast along or near the GB regions may be highly related to the GB activities including GB sliding or grain rotation due to the small grain sizes [34,38]. Even though these GB activities are insignificant during one or several cycles of deformation, the accumulation of these events during long-term fatigue tests can render the formation of the protrusions and cracks. Although the detailed damage mechanisms should be clarified through further exploration, the improvement of the cyclic softening behavior in the UFG Cu with high microstructure stability can remarkably enhance the LCF lives and then its overall fatigue properties can be improved simultaneously [25]. Therefore, the current results can provide an efficient strategy to modify the UFG structures for enhancing the fatigue properties of UFG materials that will significantly extend their prospective engineering applications.

To summarize, compared to the conventional UFG Cu obtained by SPD and the CR Cu, the cyclic softening behavior is essentially improved in the UFG Cu processed by FSP with a uniform microstructure and high microstructural stability. Typical dislocation configurations develop in some relatively large grains while the high density of dislocations can be stored in the ultrafine grains. The deformation events near the GBs lead to the formation of protrusions and cracks in the GB regions, causing the final failure.

This work was supported by the National Natural Science Foundation of China under Grants No. 51301178 and No. 51331008, the Australian Research Council (DE170100053), and the Robinson Fellowship of the University of Sydney.

Appendix A. Supplementary data

Supplementary data to this article can be found online at https://doi.org/10.1016/j.scriptamat.2019.02.040.

References

[1] R.Z. Valiev, R.K. Islamgaliev, I.V. Alexandrov, Prog. Mater. Sci. 45 (2000) 103.
[2] Y. Estrin, A. Vinogradov, Acta Mater. 61 (2013) 782.
[3] K. Lu, L. Lu, S. Suresh, Science 324 (2009) 349.
[4] E. Ma, T. Zhu, Mater. Today 20 (2017) 323.
[5] H. Mughrabi, H.W. Höppel, M. Kaulz, R.Z. Valiev, Z. Metallkd. 94 (2003) 1079–1083.
[6] H.W. Höppel, M. Korn, R. Lapovok, H. Mughrabi, Proceedings of 15th International Conference on the Strength of Materials (ICSMA 15), Dresden, August 2009, J Phys: Conf. Ser., 240, 2010, p. 012147.
[7] Y. Wang, M. Chen, F. Zhou, E. Ma, Nature 419 (2002) 912.
[8] H. Mughrabi, H.W. Höppel, Int. J. Fatigue 32 (2010) 1413.
[9] X.H. An, Q.Y. Lin, S.D. Wu, Z.F. Zhang, Mater. Res. Lett. 3 (2015) 135.
[10] H.W. Höppel, Z.M. Zhou, H. Mughrabi, R.Z. Valiev, Philos. Mag. A 82 (2002) 1781.
[11] P. Lukàš, L. Kunz, M. Svoboda, Metall. Mater. Trans. A 38 (2007) 1910.
[12] Z.J. Zhang, X.H. An, P. Zhang, M.X. Yang, G. Yang, S.D. Wu, Z.F. Zhang, Scr. Mater. 68 (2013) 389.
[13] X.H. An, S.D. Wu, Z.G. Wang, Z.F. Zhang, Acta Mater. 74 (2014) 200.
[14] R. Liu, Y.Z. Tian, Z.J. Zhang, X.H. An, P. Zhang, Z.F. Zhang, Sci. Rep. 6 (2016) 27433.
[15] R. Liu, Y.Z. Tian, Z.J. Zhang, P. Zhang, X.H. An, Z.F. Zhang, Acta Mater. 144 (2018) 613.
[16] H.W. Höppel, M. Brunnbauer, H. Mughrabi, R.Z. Valiev, A.P. Zhilyaev; in Proceedings of Materialsweek 2000, http://ww.materialsweek.org/proceedings, Munich, 2001.
[17] H.W. Höppel, R. Valiev, Z. Metallkd. 93 (2002) 641–648.

[18] R.S. Mishra, Z.Y. Ma, Mater. Sci. Eng. R 50 (2005) 1.
[19] P. Xue, B.L. Xiao, Z.Y. Ma, Mater. Des. 56 (2014) 848.
[20] J.Q. Su, T.W. Nelson, C.J. Sterling, Scr. Mater. 52 (2005) 135.
[21] P. Xue, Z.Y. Ma, Y. Komizo, H. Fujii, Mater. Lett. 162 (2016) 161.
[22] P. Xue, B.L. Xiao, Z.Y. Ma, Scr. Mater. 68 (2013) 751.
[23] C.I. Chang, X.H. Du, J.C. Huang, Scr. Mater. 57 (2007) 209.
[24] P. Xue, B.L. Xiao, Q. Zhang, Z.Y. Ma, Scr. Mater. 64 (2011) 1051.
[25] P. Xue, Z.Y. Huang, B.B. Wang, Y.Z. Tian, W.G. Wang, B.L. Xiao, Z.Y. Ma, Sci. China Mater. 7 (2016) 531.
[26] F.D. Torre, R. Lapovok, J. Sandlin, P.F. Thomson, C.H.J. Davies, E.V. Pereloma, Acta Mater. 52 (2004) 4819.
[27] L.H. Wu, X.B. Hu, X.X. Zhang, Y.Z. Li, Z.Y. Ma, X.L. Ma, B.L. Xiao, Acta Mater. 166 (2019) 371.
[28] X.W. Li, Q.W. Jiang, Y. Wu, Y. Wang, Y. Umakoshi, Adv. Eng. Mater. 10 (2008) 720.
[29] M. Goto, S.Z. Han, T. Yakushiji, S.S. Kim, C.Y. Lim, Int. J. Fatigue 30 (2008) 1333.
[30] M. Goto, S.Z. Han, K. Euh, J.H. Kang, S.S. Kim, N. Kawagoishi, Acta Mater. 58 (2010) 6249.
[31] M. Goto, K. Kamil, S.Z. Han, K. Euh, Y. Yokoho, S.S. Kim, Scr. Mater. 66 (2012) 355.
[32] X.H. An, Q.Y. Lin, S.D. Wu, Z.F. Zhang, Scr. Mater. 68 (2013) 988.
[33] S. Malekjani, P.D. Hodgson, N.E. Standord, T.B. Hilditch, Scr. Mater. 68 (2013) 821.
[34] X.H. An, S.D. Wu, Z.G. Wang, Z.F. Zhang, Prog. Mater. Sci. 101 (2019) 1.
[35] Q.S. Pan, Q.H. Lu, L. Lu, Acta Mater. 61 (2013) 1383.
[36] Q.S. Pan, L. Lu, Acta Mater. 81 (2014) 248.
[37] L.J. Jing, Q.S. Pan, J.Z. Long, N.R. Tao, L. Lu, Scr. Mater. 161 (2019) 74.
[38] S. Cheng, Y.H. Zhao, Y.M. Wang, Y. Li, X.L. Wang, P.K. Liao, E.J. Lavernia, Phys. Rev. Lett. 104 (2010) 255501.